Biochemistry and Biophysics Reports 4 (2015) 152–157

Contents lists available at ScienceDirect

Biochemistry and Biophysics Reports

journal homepage: www.elsevier.com/locate/bbrep

Biophysical and enzymatic properties of aminoglycoside adenylyltransferase AadA6 from *Pseudomonas aeruginosa*

Maria Papadovasilaki [a], Dominik Oberthür [b,1], Renate Gessmann [a], Iosifina Sarrou [a,1], Christian Betzel [b], Effie Scoulica [c,*], Kyriacos Petratos [a,*]

[a] Institute of Molecular Biology & Biotechnology, Foundation for Research & Technology-Hellas, N. Plastira 100, Heraklion 70013, Greece
[b] Laboratory for Structural Biology of Infection and Inflammation, Institute of Biochemistry and Molecular Biology, University Hamburg, Martin-Luther-King Platz 6, Hamburg 20146, Germany
[c] Laboratory of Clinical Bacteriology and Molecular Microbiology, School of Medicine, University of Crete, Voutes, Heraklion 71003, Greece

ARTICLE INFO

Article history:
Received 24 July 2015
Received in revised form
9 September 2015
Accepted 15 September 2015
Available online 18 September 2015

Keywords:
Aminoglycoside adenylyltransferase
Antibiotic modification
Circular dichroism
Enzyme kinetics
Homology modelling
Multi-angle light scattering

ABSTRACT

The gene coding for the aminoglycoside adenylyltransferase (*aadA6*) from a clinical isolate of *Pseudomonas aeruginosa* was cloned and expressed in *Escherichia coli* strain BL21(DE3)pLysS. The overexpressed enzyme (AadA6, 281 amino-acid residues) and a carboxy-terminal truncated variant molecule ([1-264] AadA6) were purified to near homogeneity and characterized. Light scattering experiments conducted under low ionic strength supported equilibrium between monomeric and homodimeric arrangements of the enzyme subunits. Circular Dichroism spectropolarimetry indicated a close structural relation to adenylate kinases. Both forms modified covalently the aminoglycosides streptomycin and spectinomycin. The enzyme required at least 5 mM $MgCl_2$ for normal Michaelis–Menten kinetics. Streptomycin exhibited a strong substrate inhibition effect at 1 mM $MgCl_2$. The truncated 17 residues at the C-terminus have little influence on protein folding, whereas they have a positive effect on the enzymic activity and stabilize dimers at high protein concentrations (>100 μM). Homology modelling and docking based on known crystal structures yielded models of the central ternary complex of monomeric AadA6 with ATP and streptomycin or spectinomycin.

1. Introduction

Antibiotic resistance of pathogenic bacteria has received immense attention over the last years as the rapid increase of multiresistant bacterial strains along with the lack of new antibiotics became a threat to global public health [1–3]. Aminoglycosides are a relatively large class of antibiotics that have been employed extensively over the past decades against aerobic bacterial pathogens [4,5]. They target accessible regions of polyanionic 16S rRNA on the 30S ribosomal subunit, notably the A site for aminoacyl-tRNA binding [6]. Following the discovery of streptomycin [7] in 1944 aminoglycosides have been widely used due to their bactericidal action and their observed synergy with other antibiotics [8]. Against this class of compounds the bacteria elaborated three mechanisms of resistance: decreased permeability of the cell wall [9], ribosome alteration [10] and enzymatic modification [11]. The latter mechanism is of most clinical importance as it confers high level of resistance and the genes encoding aminoglycoside modifying enzymes can be disseminated by plasmids or transposons [12]. Aminoglycoside modifying enzymes catalyze the modification of hydroxyl or amino groups of 2-deoxystreptamine or the sugar moieties and can be acetyltransferases (AACs), nucleotidyltranferases (ANTs), or phosphotransferases (APHs) [13]. Evolution by mutagenesis of the genes encoding the aminoglycoside modifying enzymes led to a high number of variants that can utilize an ever growing number of aminoglycoside analogues as substrates. The investigation of the function of such enzymes is expected to drive the production of efficient inhibitors that can be used in combination with the known antibiotics to reduce significantly infections by resistant pathogens. A streptomycin/spectinomycin adenylyltransferase gene (*aadA*) was first identified and sequenced [14] in *E. coli* and recently the crystal structure of an aminoglycoside adenylyltransferase (AadA) from *Salmonella enterica* has been determined at 2.5 Å resolution [15]. Herein, we

Abbreviations: [1-281]AadA6 or AadA6, full length aminoglycoside adenylyltransferase; [1-264]AadA6, genetically truncated AadA6 at the carboxy-terminus; AMPCPP, α,β-methyleneadenosine 5′-triphosphate; MALS, Multi-angle light scattering; MIC, Minimum Inhibitory Concentration

* Corresponding authors.
E-mail addresses: scoulica@med.uoc.gr (E. Scoulica), petratos@imbb.forth.gr (K. Petratos).
[1] Present address: Center for Free-Electron Laser Science, Deutsches Elektronen Synchrotron-DESY, Notkestrasse 85, Hamburg 22607, Germany.

http://dx.doi.org/10.1016/j.bbrep.2015.09.011

investigated the protein encoded by the gene *aadA6* identified in a clinical multiresistant isolate of *P. aeruginosa* Ps100 located in the integron In118 [16,17]. The protein termed AadA6 belongs to the subclass of 3″-O-nucleotidyltransferases (*ANT*3″), it consists of 281 amino-acid residues (UniProt: Q9RGC2) and confers resistance to streptomycin and spectinomycin [16]. The sequence information collected from the Conserved Domain Database (CDD) [18] for this protein points to the conserved nucleotidyltransferase (NTase) domain lying between residues 10 and 110. This domain includes the nucleotide triphosphate binding site and one Mg^{2+} binding site [19, 20].

In the present work circular dichroism spectra, laser light scattering and kinetic data have been measured for purified AadA6 and a C-terminal truncated variant of the enzyme. The latter was termed [1-264]AadA6 and was produced in an attempt to achieve an enzyme form easier to crystallize than the wild type. Finally, two theoretical models of the structures of the AadA6 ternary complexes with ATP and streptomycin or spectinomycin were built based on the homologous AadA from *S. enterica* [15].

2. Materials and methods

2.1. Gene cloning

Total DNA from the *P. aeruginosa* strain Ps100 was purified by QIAamp DNA mini kit (Qiagen, Germany) and used in order to amplify the coding sequence of the *aadA6* gene by PCR. The primers were designed according to sequence information obtained by direct sequencing of the *aadA*6 gene containing integron of the *P. aeruginosa* strain Ps100 as described previously [21] (GenBank: AY460181). The PCR products were purified by the Jetquick kit (Genomed, Germany) were digested with the *Nde*I/*Bam*HI endonucleases and ligated in the corresponding restriction sites of the pT7-7 (amp^r) expression vector. The recombinant plasmids were transformed in *E. coli* BL21(DE3) pLysS cells. Transformed bacteria were grown in Luria-Bertani (LB) medium containing 100 μg/ml ampicillin and 34 μg/ml chloramphenicol. The site of insertion of the PCR products was confirmed by Sanger sequencing of the purified recombinant plasmids (Macrogen, Europe).

2.2. Protein expression and purification

Four liters of LB medium containing 1 mM $MgCl_2$ were inoculated with 40 ml of an overnight culture of each of the recombinant strains and let grow under shaking at 220 rpm (37 °C). When the absorbance at 600 nm reached 0.5–0.8 the temperature was decreased to 18 °C and growth continued for 16 more hours in the presence of 0.3 mM isopropyl β-D-1-thiogalactopyranoside (IPTG). 16 g of cell paste was resuspended in 16 ml lysis buffer (50 mM Tris–HCl pH 7.5, 50 mM NaCl) containing 4 mM mercaptoethanol and 2 mM $MgCl_2$. Lysozyme was added to 0.3 mg/ml followed by very gentle stirring on ice for 1.5 h. Following centrifugation the soluble fraction was applied on a 30 ml Q-Sepharose™ matrix (GE Healthcare, Piscataway, NJ, USA). The bound protein was eluted with a NaCl gradient. Appropriate fractions were combined and applied on a 20 ml Hydroxyapatite™ matrix (Bio-Rad Laboratories, Hercules, CA, USA). The bound enzyme was eluted with a KH_2PO_4/Na_2HPO_4 pH 7.2 gradient. Finally, fractions that eluted with approximately 13 mM $KH_2PO_4/NaHPO_4$ were applied on an S-100 Sephacryl HR™ gel filtration column (GE Healthcare). Samples from all steps of a purification experiment were run with SDS-PAGE. Based on the latter analytical method selected fractions were combined and concentrated.

2.3. In vitro enzymatic activity

Steady-state enzyme kinetics monitored the phosphate as end-product of the adenylyltransferase action combined with that of inorganic pyrophosphatase. The analytical method employed was a modification of the colorimetric method based on the reaction of malachite green, molybdates and phosphates [22,23]. The initial rates were measured in reaction mixtures of 65 nM enzyme and varying substrate concentrations in 50 mM Tris–HCl pH 7.5 buffer containing 15 mM $MgCl_2$ at 23 °C. In the earlier experiments 1, 5 and 10 mM $MgCl_2$ were also present during the kinetic analyses. Each reaction was stopped at the selected time intervals by addition of 26 μl 2.25N H_2SO_4. After standing for 10 min at 0 °C, the mixture was centrifuged for 3 min in order to remove the protein and the supernatant was taken for phosphate determination. The antibiotic substrates spectinomycin and dihydrostreptomycin varied from 2–20 μM. ATP varied from 20–120 and 20–160 μM when spectinomycin and dihydrostreptomycin were analysed, respectively. Pre-incubation of all reaction components except the analysed enzyme was performed for 10 min. The latter procedure allowed the consumption of probable endogenous phosphates so that they did not interfere with the measurements of enzyme activity. All kinetic data were collected in triplicates. Oxidized streptomycin was also tested though in a limited number of reactions and showed the same kinetic behaviour with its reduced counterpart.

2.4. Data analysis

Based on earlier results for a closely related enzyme [24] the same steady-state assumption was made for sequential ordered bi-substrate reactions. In this case, Eq. (1) provides the initial velocities and was fitted with the measured initial rates when both substrates were varied. Non-linear fits of the data to Eq. (1) were carried out using Grafit 7.0 (Erithacus Software Ltd., Horley, U.K.).

$$v = V_{max}[A][B]/\left(K_{ia}K_{m_b} + K_{m_b}[A] + K_{m_a}[B] + [A][B]\right) \quad (1)$$

In the above equation, v is the initial velocity, V_{max} is the maximal velocity, K_{m_a} and K_{m_b} are the Michaelis–Menten constants of substrates A and B, respectively and K_{ia} is the dissociation constant of the first substrate *A* that is added to the enzyme. In the present analysis, *A* and *B* refer to ATP and streptomycin or spectinomycin, respectively.

2.5. Biophysical characterization

Circular Dichroism spectropolarimetry measurements of the two forms of the purified enzyme were conducted with a J-810 spectropolarimeter (JASCO, Inc., USA). The data were processed using both software and reference databases of the DichroWeb server [25]. For the recording of the spectra protein solutions of 0.2 mg/ml were used in 50 mM potassium phosphate buffer pH 7.5 whereas for the thermal unfolding experiments solutions of 0.1 mg/ml were prepared in the same buffer. During the melting experiments the ellipticities (θ) at wavelength 209 nm corresponding to the minimum value of the spectra, were recorded with increasing temperature. CD data for the full-length AadA6 and truncated enzyme [1-264]AadA6 have been deposited in the Protein Circular Dichroism Data Bank (PCDDB) [26] with PCDDB id codes: CD0004574000 and CD0004575000, respectively.

The dynamic light scattering [27] of samples containing approximately 4 mg/ml of enzyme were analysed in 50 mM Tris–HCl pH 7.5 buffer solutions with two concentrations of $MgCl_2$ (1 and 18 mM for AadA6, 1 and 15 mM for [1-264]AadA6) at 20 °C with the HELEOS8 MALS (Multi-angle light scattering) instrument

(Wyatt Technology Corp., Santa Barbara, CA, USA). The instrument operated in combination with a Superdex 200HR 10/30 prepacked gel filtration column (GE Healthcare). The light scattering experiments were carried out also in the presence of 2 mM of both AMPCPP and streptomycin. The quasi-elastic scattering data along with the refractive index and UV absorbance measurements were analysed with software ASTRA® 6.1.117. This analysis allowed also the estimation of the molecular masses of the eluates and thus the assignment of the correct oligomeric state of the protein.

2.6. Homology modelling

A model for the structure of AadA6 (3-262) was obtained from the Swiss-Model protein server [28] based on the homologous AadA (identity ~45%) from *S. enterica* (PDB: 4CS6), which served as template. For this model, a structural alignment of the N-terminal domain of AadA with chain A of kanamycin nucleotidyltransferase (KNTase) (PDB: 1KNY) was generated, overlapping mainly the β-strands in this domain. The aim of the latter alignment was to locate the ATP and aminoglycoside binding sites. The structural alignment showed that there are certain characteristic substrate binding residues in AadA like in KNTase. This allowed the placement of the substrates ATP and streptomycin to the corresponding binding sites in KNTase. Finally, the model was energy minimized with the program CNS [29] using coordinates and modified geometrical restraint files from the HIC-Up database (xray.bmc.uu.se/hicup/, [30]). The coordinates of the derived AadA6 theoretical model are available at the Model Archive (www.modelarchive.org/) under accession number MA-AWT7Q. In addition, a second model of AadA6 was derived with ATP and spectinomycin in the enzyme's active site following analogous procedures as described above.

3. Results

3.1. Strains and antibiotic profile

Clinical strain Ps100 was highly resistant against streptomycin, gentamycin and amikacin [MIC (Minimum Inhibitory Concentration) > 256 μg/ml], while the recombinant *E. coli* strains expressing either the full length or the truncated AadA6 exhibited resistance against streptomycin but not gentamycin or amikacin, indicating that the resistant phenotype was conferred by the corresponding determinant. The MIC values for streptomycin were determined by the broth dilution method at 730 and 315 μg/ml for the *E. coli* BL21[1-281] and BL21[1-264] strains, respectively. We assigned the observed differences to the distinct expression levels (see Section 3.2) and activities (see Section 3.3) of the two proteins.

3.2. Protein expression and purification

On average 16 g of cell pellet yielded about 7 mg of both 95% pure AadA6 and 98% pure [1-264]AadA6. This was invariably observed despite the approximately half level of expression of [1-264]AadA6 compared to that of AadA6.

3.3. Enzymatic characterization

AadA6 exhibits high degree of sequence identity (264/268 residues) to the nucleotidyltransferase domain [ANT(3″)-Ii] of the bifunctional, nucleotidyl- and acetyl-transferase aminoglycoside modifying enzyme from *Serratia marcescens* (UniProt: Q8VQN7), which has been extensively characterized with regard to its enzymatic properties [24]. The high homology between the enzymes suggests that AadA6 acts in a similar fashion. We decided to purify the truncated form of AadA6 based on the length of the above mentioned closely related domain of the bifunctional enzyme and on the results of sequence comparisons with other homologous proteins [31] using the Universal Protein Resource Knowledgebase. Enzymatic assays of product inorganic pyrophosphate using streptomycin as substrate provided specific activities of 1.3 ± 0.1 and 0.9 ± 0.1 μmol min^{-1} mg^{-1} for homogeneous samples of AadA6 and [1-264]AadA6, respectively. The latter values indicate that the truncated enzyme is about 70% as active as the original full-length enzyme in vitro. The observed decrease of activity is due to the truncation of the 17C-terminal residues. The active site comprises mainly N-terminal residues according to the theoretical models described below (Section 3.5). The determined kinetic parameters for AadA6 are summarized in Table 1. These results agree to the earlier reported values for the bifunctional enzyme [24] except of the K_m value for spectinomycin, which was calculated to be about four times lower. This leads to a five-fold higher specificity of AadA6 for spectinomycin comparing to the highly homologous enzyme from *S. marcescens*.

Table 1
Steady-state kinetic parameters of aminoglycoside adenylyltransferase and its engineered variant.

	Substrate	k_{cat} (s^{-1})	K_m (μM)	k_{cat}/K_m ($M^{-1}s^{-1}$)
AadA6	streptomycin	0.66 ± 0.06	1.8 ± 0.6	$(3.7 \pm 1.3) \times 10^5$
	spectinomycin	0.63 ± 0.03	0.4 ± 0.1	$(1.6 \pm 0.4) \times 10^6$
	ATP	0.61 ± 0.03	11.0 ± 1.2	$(5.5 \pm 0.7) \times 10^4$
[1-264]AadA6	streptomycin	0.47 ± 0.04	3.3 ± 0.7	$(1.4 \pm 0.3) \times 10^5$
	spectinomycin	0.26 ± 0.02	0.2 ± 0.1	$(1.3 \pm 0.7) \times 10^6$
	ATP	0.41 ± 0.02	10.5 ± 0.8	$(3.9 \pm 0.4) \times 10^4$

Moreover, kanamycin A, gentamycin, and amikacin were also tested as substrates for AadA6 with no detectable rates of reaction. Kanamycin A was actually found to be competitive inhibitor for the aminoglycoside substrates.

Finally, it is worth noting that when the initial velocity measurements were carried out in the presence of 1 mM $MgCl_2$ a strong substrate inhibition effect was invariably observed by streptomycin. This was largely alleviated by increasing the concentration of $MgCl_2$ to 5 mM. An analogous Mg^{2+} concentration effect was also observed in the case of kanamycin nucleotidyltransferase [32] as well as other aminoglycoside adenylyltransferases [33].

3.4. Biophysical characterization

Analysis of the far-UV (190–240 nm) CD-spectra shown in Fig. 1A provided for AadA6 58% α-helical and 19% β-sheet content. The respective values for [1-264]AadA6 were 52% and 23%. The CD spectra of AadA6 revealed remarkable similarity to that of adenylate kinase (PDB: 3ADK), which is used in various reference data sets for the estimation of secondary structure by CD spectroscopy.

In order to probe the thermal denaturation of both forms of the enzyme, CD measurements were conducted as function of temperature (Fig. 1B). The melting temperatures (T_m) for AadA6 and [1-264]AadA6 were estimated by interpolation on the melting curves as 49.5 and 51.0 ± 0.5 °C, respectively. The thermal unfoldings of the full-length and truncated enzymes were found to occur in one irreversible step.

In addition, laser light scattering experiments were carried out for both AadA6 and [1-264]AadA6 in combination with an analytical gel filtration column. The results of two selected experiments are shown in Fig. 2 and a complete list of the derived molecular hydrodynamic radii is given in Table 2.

All light scattering measurements support equilibrium between

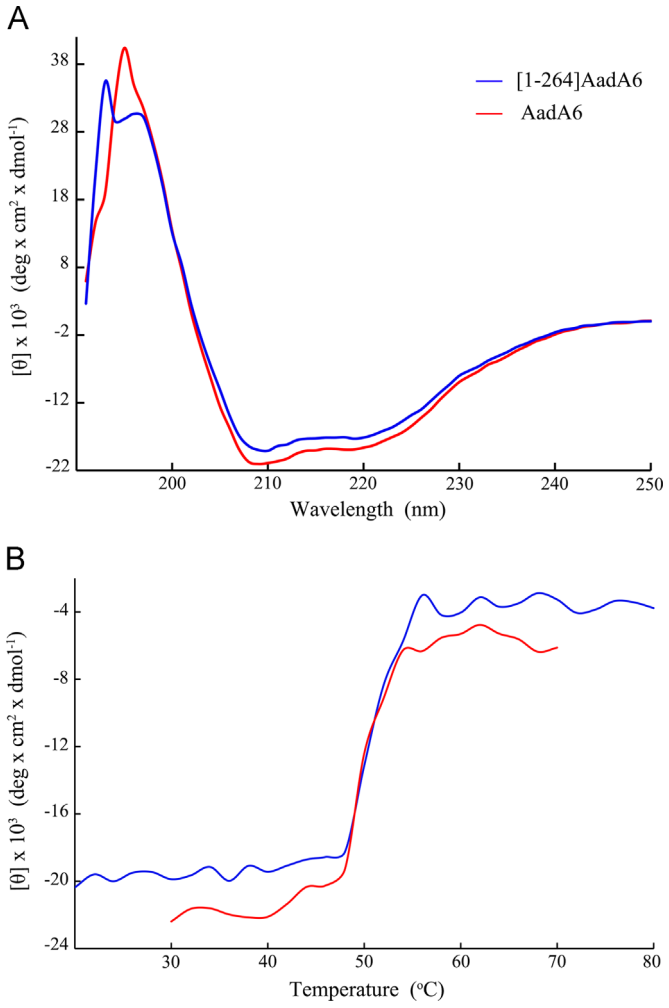

Fig. 1. Circular Dichroism spectropolarimetry data and thermal denaturation curves. (A) Far-UV CD spectra of AadA6 (red) and [1-264]AadA6 (blue) were recorded at 10 °C. (B) Superimposed thermal melting CD curves for both proteins are labelled as in (A). The ordinates of both plots present values of mean residue ellipticity [θ].

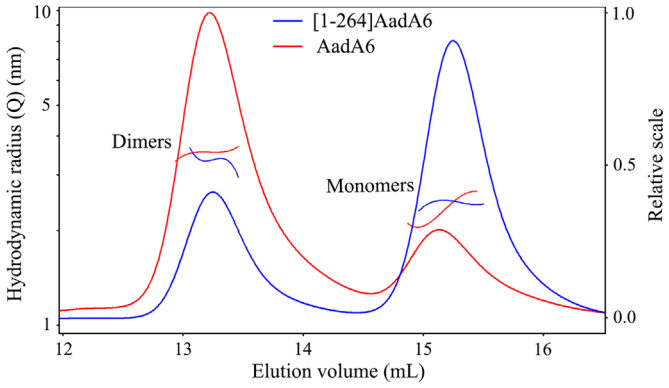

Fig. 2. Multi-angle light scattering (MALS) curves. Relative quasi-elastic light scattering intensities (right axis) of AadA6 (red) and [1-264]AadA6 (blue) in 50 mM Tris–HCl pH 7.5 buffer at 1 mM $MgCl_2$ as function of their elution volumes from an analytical gel-filtration column. The two peaks correspond to the dimer and monomer of each protein. The estimates of the respective molecular hydrodynamic radii (R_H) as function of volume slice are also shown. The plots were produced by the data analysis software provided by the instrument manufacturer.

dimeric and monomeric species of AadA6, with mean hydrodynamic radii of 3.4 ± 0.1 and 2.2 ± 0.2 nm, respectively. The same holds true for [1-264]AadA6 with respective values 3.3 ± 0.1 and 2.4 ± 0.1 nm. Addition of $MgCl_2$ and substrate or substrate analogues led to a decrease of the apparent size of the proteins. The latter effect was more prominent for the monomeric form of AadA6. MALS data collected from solutions with ionic strength values of 60–150 mM showed that AadA6 is in equilibrium with an approximate 1:1 dimer to monomer ratio whereas the corresponding value for [1-264]AadA6 was about 1:4. This latter observation indicates that the deleted C-terminal residues favour the formation of protein dimers at concentrations approximately 100 μM used in these light scattering experiments. The occurrence of monomers is in agreement with the recently reported structure of AadA from *S. enterica* [15].

Table 2
Average hydrodynamic radii (R_H) of AadA6 and [1-264]AadA6 based on multi-angle light scattering experiments.

AadA6	AMPCPP[a]	Streptomycin[a]	Dimer R_H (nm)	Monomer R_H (nm)
1 mM $MgCl_2$			3.4 ± 0.1	2.2 ± 0.2
	+	+	3.3	2.0
18 mM $MgCl_2$			2.9	1.9
	+	+	3.3	1.5
[1-264] AadA6				
1 mM $MgCl_2$			3.3 ± 0.1	2.4 ± 0.1
	+	+	3.4	2.4
15 mM $MgCl_2$			3.2	2.5
	+	+	3.0	2.4

[a] AMPCPP and streptomycin were added each at 2 mM concentrations.

Moreover, the ionic strength seems to influence the dimerization of the molecule. Light scattering experiments of ~400 μM [1-264]AadA6 in high ionic strength solutions (~350 mM) showed that the protein is dimeric (data not shown). This finding is in agreement with the reported structures of the distantly related (identity <20%) kanamycin nucleotidyltransferase [20] from *S. aureus* (PDB: 1KNY) and aminoglycoside 4′-O-adenylyltransferase [ANT(4′)-IIb] from *P. aeruginosa* (PDB: 4EBJ).

3.5. Homology modelling

Two theoretical models were constructed for the structures of AadA6 with ATP and streptomycin or spectinomycin. Both comprise two structural domains that are in the 'closed' state similar to the starting model (PDB: 4CS6) and different to the kanamycin nucleotidyltransferase (KNTase) structure. In the latter case an 'open' state of the domains was reported, which facilitates the formation of the observed dimers in the KNTase structure. First, the bound substrates ATP and streptomycin were also modelled based on the structure of the KNTase ternary complex with AMPCPP and kanamycin. Second, a model was obtained for the ternary complex of AadA6:ATP:Spectinomycin. A close-up view of the modelled active site region of the first structure with both substrates bound is shown in Fig. 3. In the latter figure are shown most of the interactions except those between the bound ATP and Ser46, Asp130 and Tyr231. There are three H-bonds between streptomycin and the enzyme. There was also found one H-bond between ATP and streptomycin. Residues of the N-terminal domain (1-157) constitute mainly the active site of the enzyme. The C-terminal domain contributes only three residues when streptomycin was modelled, namely Asn185 that H-bonds to streptomycin and Lys205, Tyr231 that H-bond to ATP. Fig. S1 of the Supplementary section shows a close-up view of the second modelled structure in an analogous content and orientation. In this Figure the two additional H-bonds of spectinomycin with the enzyme are shown, namely those with Gln108 and Asp182. This additional interaction may provide an explanation for the higher specificity of AadA6 for spectinomycin.

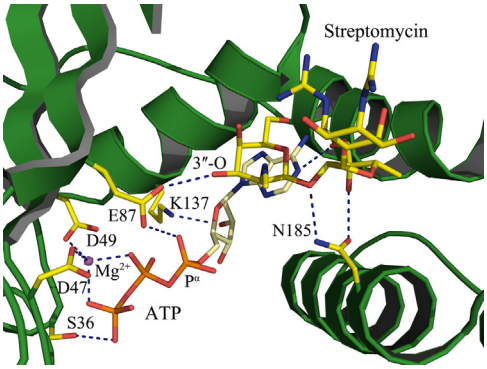

Fig. 3. Theoretical modelling of AadA6 structure. Active site view with both ATP and streptomycin. The crystal structures used as templates were, AadA from *S. enterica* (PDB: 4CS6) and kanamycin nucleotidyltransferase from *S. aureus* (PDB: 1KNY). The labelled protein residues that interact with the substrates are shown in stick representation (atom colours, carbon: yellow for streptomycin and light yellow for ATP, nitrogen: blue, oxygen: red, phosphorus: orange). The sphere in magenta denotes the magnesium ion. The dashes indicate H-bonding or the co-ordination of the magnesium ion. The figure was prepared with PyMOL (http://www.pymol.org).

4. Discussion

The enzyme kinetic experiments presented in this work for AadA6 from *P. aeruginosa* and its truncated variant [1-264]AadA6 revealed clear and measurable deviation of the catalytic activity between the two forms. AadA6 was found to be about 40% more active than [1-264]AadA6 in modifying streptomycin indicating that the 17 residues at the C-terminus, which are missing in [1-264]AadA6 are necessary for full activity. The same 17C-terminal residues also support protein dimerization at high enzyme concentrations ($>100\ \mu M$) as is derived from MALS experiments contacted under ionic strength conditions (60–150 and 350 mM) close to the physiological values (>100 mM) [34]. Moreover, AadA6 exhibits higher specificity for spectinomycin, which is retained in the truncated form. The higher specificity for spectinomycin compared to streptomycin may be explained theoretically as follows. The model derived for the structure of the complex of AadA6 with ATP and spectinomycin shows five H-bonds between the enzyme and the antibiotic whereas the respective H-bonds with streptomycin are only three. This leads to a better binding of spectinomycin compared with streptomycin and thus higher specificity for spectinomycin. In the presence of 1 mM $MgCl_2$ used in the early experiments a prominent substrate inhibition was observed with streptomycin for concentrations greater than 3 μM. It is noteworthy that this $MgCl_2$ concentration lies close to the reported physiological values of uncomplexed, free magnesium ions (0.9–1.5 mM) for the *S. enterica* [35]. Substrate inhibition as well as the decrease of the protein size observed with the MALS experiments may be due to a more general binding of Mg^{2+} with this acidic enzyme (theoretical pI ~5.0). Non-specific Mg^{2+} binding may eliminate a potential non-productive binding of streptomycin to the negatively charged pocket of the active site [15] leading thus to the observed normal Michaelis–Menten kinetics. Furthermore, partial neutralization of the negative charges on the protein surface could result in a more compactly folded structure with the observed smaller hydrodynamic radius. Further work is necessary for the elucidation of the general effect of magnesium ions. This will provide a thorough explanation of the phenomenon and help towards the rational design of AadA6 inhibitors.

The determined kinetic parameters are in agreement with the results for the closely related nucleotidyltransferase domain of the bifunctional enzyme from *S. marcescens* [24]. The only notable difference is the specificity constant for spectinomycin, which for AadA6 was about five times greater. The authors cannot provide a plausible explanation for this observation due to the absence of any structures for the bifunctional enzyme.

In the proposed model of the ternary complex with ATP and streptomycin the distance of the 3″-O of streptomycin is about 6 Å from the α-phosphorus (P^{α}) of ATP (Fig. 3). This structure after rearrangement could lead eventually to a nucleophilic attack on the P^{α} of ATP resulting in the transfer of its adenyl moiety to the 3″-hydroxyl group of streptomycin. The reaction may be facilitated by the nearby residue Glu87 acting as catalytic base. Analogous arguments hold true for spectinomycin although its oxygen O-9 subject to adenylation is modelled even further away (6.8 Å) from the α-phosphorus of ATP. The proposed models show the potential rearrangement of the ternary complexes and give insight on the catalytic activity of AadA6. This latter activity is required for the herein presented kinetic experiments at a low enzyme concentration (65 nM), which justifies for the exclusive presence of the monomeric form. A different arrangement of the substrates may be possible on two cooperating active sites in case the enzyme is to function as dimer.

Sequence comparisons suggest that AadA6 belongs to the superfamily of ancient nucleotidyltransferases involved in diverse biological functions that range from DNA repair to regulation of biosynthetic pathways and antibiotic resistance [36]. Detailed structure comparisons with members of this superfamily have to wait for the determination of the three-dimensional structure of AadA6 under various conditions.

Finally, the herein described biochemical and biophysical properties along with the supplied structural models provide insight for substrate binding with AadA6 and may facilitate future attempts to design inhibitors that will allow the re-usage of the first generation antibiotics like the aminoglycosides against multiresistant pathogens.

5. Note

This paper is dedicated to the memory of our late colleague Dr. Yannis Papanikolau who had generously advised us on the protein purification procedures.

Acknowledgements

We thank Prof. Vassilis Bouriotis and Dr. Efstratios Mylonas for their insightful comments. We also thank Mr. Nikos Kountourakis of the Proteomics Facility of IMBB-FORTH for scanning SDS-PAGE gels. In particular, we are grateful to Prof. Electra Gizeli and her laboratory staff for the use of the microplate reader. This work was funded by the EU Programme FP7-REGPOT-2012 InnovCrete (Grant agreement no. 316223). I.S. acknowledges support also from InnovCrete. This work was performed in part in the framework of the BIOSYS research project, Action KRIPIS, project no. MIS-448301 (Grant no. 2013SE01380036), which was funded by the General Secretariat for Research and Technology, Ministry of Education, Greece, and the European Regional Development Fund (Sectoral Operational Programme: Competitiveness and Entrepreneurship, NSRF 2007–2013)/European Commission.

Appendix A. Supplementary material

Supplementary data associated with this article can be found in the online version at http://dx.doi.org/10.1016/j.bbrep.2015.09.011.

References

[1] N.E. Holmes, B.P. Howden, The rise of antimicrobial resistance: a clear and present danger, Expert Rev. Anti Infect. Ther. 9 (2011) 645–648.
[2] D.M. Livermore, Current epidemiology and growing resistance of gram-negative pathogens, Korean J. Intern. Med. 27 (2012) 128–142.
[3] M. Perros, Infectious disease. A sustainable model for antibiotics, Science 347 (2015) 1062–1064.
[4] B.D. Davis, Mechanism of bactericidal action of aminoglycosides, Microbiol. Rev. 51 (1987) 341–350.
[5] S.B. Vakulenko, S. Mobashery, Versatility of aminoglycosides and prospects for their future, Clin. Microbiol. Rev. 16 (2003) 430–450.
[6] A.P. Carter, W.M. Clemons, D.E. Brodersen, R.J. Morgan-Warren, B.T. Wimberly, V. Ramakrishnan, Functional insights from the structure of the 30S ribosomal subunit and its interactions with antibiotics, Nature 407 (2000) 340–348.
[7] W. Piepersberg, Streptomycin and related aminoglycosides, Biotechnology 28 (1995) 531–570.
[8] H. Giamarellou, N.P. Zissis, G. Tagari, J. Bouzos, In vitro synergistic activities of aminoglycosides and new beta-lactams against multiresistant *Pseudomonas aeruginosa*, Antimicrob. Agents Chemother. 25 (1984) 534–536.
[9] R.A. Hatch, N.L. Schiller, Alginate lyase promotes diffusion of aminoglycosides through the extracellular polysaccharide of mucoid *Pseudomonas aeruginosa*, Antimicrob. Agents Chemother. 42 (1998) 974–977.
[10] M.P. Mingeot-Leclercq, Y. Glupczynski, P.M. Tulkens, Aminoglycosides: activity and resistance, Antimicrob. Agents Chemother. 43 (1999) 727–737.
[11] S. Jana, J.K. Deb, Molecular understanding of aminoglycoside action and resistance, Appl. Microbiol. Biotechnol. 70 (2006) 140–150.
[12] A.C. Fluit, F.J. Schmitz, Resistance integrons and super-integrons, Clin. Microbiol. Infect. 10 (2004) 272–288.
[13] G.D. Wright, Aminoglycoside-modifying enzymes, Curr. Opin. Microbiol. 2 (1999) 499–503.
[14] S. Hollingshead, D. Vapnek, Nucleotide sequence analysis of a gene encoding a streptomycin/spectinomycin adenylyltransferase, Plasmid 13 (1985) 17–30.
[15] Y. Chen, Structural and Biochemical Studies of Antibiotic Resistance and Ribosomal Frameshifting, Acta Universitatis Upsaliensis, Uppsala, 2013.
[16] T. Naas, L. Poirel, P. Nordmann, Molecular characterisation of In51, a class 1 integron containing a novel aminoglycoside adenylyltransferase gene cassette, aadA6, in *Pseudomonas aeruginosa*, Biochim. Biophys. Acta 1489 (1999) 445–451.
[17] C.G. Giske, B. Libisch, C. Colinon, E. Scoulica, L. Pagani, M. Fuzi, G. Kronvall, G. M. Rossolini, Establishing clonal relationships between VIM-1-like metallo-beta-lactamase-producing *Pseudomonas aeruginosa* strains from four European countries by multilocus sequence typing, J. Clin. Microbiol. 44 (2006) 4309–4315.
[18] A. Marchler-Bauer, S. Lu, J.B. Anderson, F. Chitsaz, M.K. Derbyshire, C. DeWeese-Scott, J.H. Fong, L.Y. Geer, R.C. Geer, N.R. Gonzales, M. Gwadz, D. I. Hurwitz, J.D. Jackson, Z. Ke, C.J. Lanczycki, F. Lu, G.H. Marchler, M. Mullokandov, M.V. Omelchenko, C.L. Robertson, J.S. Song, N. Thanki, R. A. Yamashita, D. Zhang, N. Zhang, C. Zheng, S.H. Bryant, CDD: a Conserved Domain Database for the functional annotation of proteins, Nucleic Acids Res. 39 (2011) D225–D229.
[19] J. Sakon, H.H. Liao, A.M. Kanikula, M.M. Benning, I. Rayment, H.M. Holden, Molecular structure of kanamycin nucleotidyltransferase determined to 3.0-A resolution, Biochemistry 32 (1993) 11977–11984.
[20] L.C. Pedersen, M.M. Benning, H.M. Holden, Structural investigation of the antibiotic and ATP-binding sites in kanamycin nucleotidyltransferase, Biochemistry 34 (1995) 13305–13311.
[21] E.V. Scoulica, I.K. Neonakis, A.I. Gikas, Y.J. Tselentis, Spread of bla(VIM-1)-producing *E. coli* in a university hospital in Greece. Genetic analysis of the integron carrying the bla(VIM-1) metallo-beta-lactamase gene, Diagn. Microbiol. Infect. Dis. 48 (2004) 167–172.
[22] A.A. Baykov, V.N. Kasho, S.M. Avaeva, Inorganic pyrophosphatase as a label in heterogeneous enzyme immunoassay, Anal. Biochem. 171 (1988) 271–276.
[23] T.P. Geladopoulos, T.G. Sotiroudis, A.E. Evangelopoulos, A malachite green colorimetric assay for protein phosphatase activity, Anal. Biochem. 192 (1991) 112–116.
[24] C. Kim, D. Hesek, J. Zajicek, S.B. Vakulenko, S. Mobashery, Characterization of the bifunctional aminoglycoside-modifying enzyme ANT(3″)-Ii/AAC(6′)-IId from Serratia marcescens, Biochemistry 45 (2006) 8368–8377.
[25] L. Whitmore, B.A. Wallace, Protein secondary structure analyses from circular dichroism spectroscopy: methods and reference databases, Biopolymers 89 (2008) 392–400.
[26] L. Whitmore, B. Woollett, A.J. Miles, D.P. Klose, R.W. Janes, B.A. Wallace, PCDDB: the Protein Circular Dichroism Data Bank, a repository for circular dichroism spectral and metadata, Nucleic Acids Res. 39 (2011) D480–D486.
[27] K.S. Schmitz, An Introduction to Dynamic Light Scattering of Macromolecules, Academic Press, New York, 1990.
[28] K. Arnold, L. Bordoli, J. Kopp, T. Schwede, The SWISS-MODEL workspace: a web-based environment for protein structure homology modelling, Bioinformatics 22 (2006) 195–201.
[29] A.T. Brunger, P.D. Adams, G.M. Clore, W.L. DeLano, P. Gros, R.W. Grosse-Kunstleve, J.S. Jiang, J. Kuszewski, M. Nilges, N.S. Pannu, R.J. Read, L.M. Rice, T. Simonson, G.L. Warren, Crystallography & NMR system: a new software suite for macromolecular structure determination, Acta Crystallogr. D54 (1998) 905–921.
[30] G.J. Kleywegt, K. Henrick, E.J. Dodson, D.M.F. van Aalten, Pound-wise but penny-foolish – How well do micromolecules fare in macromolecular refinement? Structure 11 (2003) 1051–1059.
[31] S.F. Altschul, W. Gish, W. Miller, E.W. Myers, D.J. Lipman, Basic local alignment search tool, J. Mol. Biol. 215 (1990) 403–410.
[32] M. Chen-Goodspeed, J.L. Vanhooke, H.M. Holden, F.M. Raushel, Kinetic mechanism of kanamycin nucleotidyltransferase from Staphylococcus aureus, Bioorg. Chem. 27 (1999) 395–408.
[33] E. Azucena, S. Mobashery, Aminoglycoside-modifying enzymes: mechanisms of catalytic processes and inhibition, Drug Resist. Updat. 4 (2001) 106–117.
[34] J. Spitzer, B. Poolman, The role of biomacromolecular crowding, ionic strength, and physicochemical gradients in the complexities of life's emergence, Microbiol. Mol. Biol. Rev. 73 (2009) 371–388.
[35] E.M. Froschauer, M. Kolisek, F. Dieterich, M. Schweigel, R.J. Schweyen, Fluorescence measurements of free [Mg^{2+}] by use of mag-fura 2 in *Salmonella enterica*, FEMS Microbiol. Lett. 237 (2004) 49–55.
[36] L. Holm, C. Sander, DNA polymerase beta belongs to an ancient nucleotidyltransferase superfamily, Trends Biochem. Sci. 20 (1995) 345–347.